Medical Image Retrieval Based on An Improved Non-negative Matrix Factorization Algorithm

J. Wang[1*], S.Y. Lai[2], M.D. Li[1], D. H. Lies[3]
[1]College of Computers, China West Normal University
[2]Department of Medical Imaging, North Sichuan Medical College Nanchong, 637000, China
[3]Department of Information Engineering, SCUT, Radlinského 109 Koice, Slovakia
wjuan0712@126.com

JDIM
Journal of Digital Information Management

ABSTRACT: *A gradient-projected relevance feedback algorithm based on non-negative matrix factorization (NMF) is proposed in this study to improve the performance of retrieval algorithm in the medical image processing field. Relevance feedback has been an important method in image retrieval technology in recent years because it allows users to participate. Thus, it can compensate for the shortcomings of using low-level features to describe the semantic contents of an image to some degree. Given that NMF can partly sketch the distribution of relevant images in the space represented by the base matrix, finding more related images from image repositories is possible. This condition can be achieved by conducting an NMF operation of the query image, using the gradient projection iterative rules to update variables, and selecting the appropriate iteration stop conditions to optimize the time complexity of the algorithm. Compared with the commonly used and multiplicative updating NMF approaches, the proposed method improved the speed of the feedback on the premise of guaranteeing precision and recall rates, and significantly optimized the retrieval accuracy. Experiments were conducted on the base of 586 cerebral hemorrhage images and 634 spine and cervical-spine mixed images. Results show that the proposed approach is feasible in medical image retrieval.*

Subject Categories and Descriptors
I.5.3 [Clustering]: Algorithms; **H.2.8 [Database Applications]:** Image databases

General Terms: Computational Complexity, Similarity Measures, Matrix Factorization, Annotation

Keywords: Gradient Projection, Medical Image Retrieval, Relevance Feedback, Non-negative Matrix Factorization

Received: 18 July 2015, Revised 21 August 2015, Accepted 27 August 2015

1. Introduction

Content-based image retrieval has been one of the most active research areas in recent years [1]. With regard to the traditional feature extraction- and the similarity distance-based methods, a significant gap may exist between the auto-extracted image features and the semantic perception of humans, thereby potentially leading to unsatisfactory retrieval results. The use of relevance feedback changes the results. The basic idea of the relevance feedback method allows users to annotate and evaluate the results in the retrieval process, and indicate the returned images that are relevant or not to the query images. The relevant information annotated by users is used as training samples and reported back to the system to join the next round of retrieval, which will make the retrieval results more consistent with the needs of the user.

With the wide use of medical imaging devices in clinical applications, a large number of medical images, especially digital images, are produced per day in the medical field. Consequently, high effective management on these images and application on clinical diagnostics and therapy are becoming emergent problems that should be addressed. Given the limitations of manual annotation, content-based medical image retrieval (CBMIR) technology

has received increasing attention. CBMIR is different from CBIR because the former must consider medical context, such as subtle artifacts or pathological changes [2]. In the past decades, varied CBMIR systems have been developed based on specified medical tasks. These systems include not only the system that aims to solve the images based on pathology, ecsomatics, and medical imaging, but also the medical image retrieval experiment system. Studies [3][4] introduced the classification of skin disease based on CBMIR. The literature [5] also described a method that was used to retrieve pathological tuberculosis pictures. Korn developed a CBMIR system that focuses on breast tumor examination [6]. Both Institute TELECOM [7] and Bu Ali Sina University [8] conducted extensive research on computer-aided diagnosis and related software development. Table 1 shows several types of the CBMIR system.

Function / Image Types	Names of the System
Lung HRCT	ASSERT
Image Classification	MedGIFT, ImageEngine
Pathology Images	PathFinder, PathMaster
Biology Images	BioImage, BIRN
Dermatology	MELDOQ, MEDS
X-ray Images on Spine	CBIR2, MIRS
	IDEM, I-Browse

Table 1. Classification of Medical Images and Related CBIR System

In relevance feedback algorithm frameworks related to non-negative matrix factorization (NMF) [9][10][11][12], the positive samples annotated by users constitute the sample characteristic matrix. The base and the coefficient matrices can both be obtained in each feedback round by conducting NMF decomposition, which is called the NMF decomposition model. Hence, the model can be considered as the base for image retrieval. For typical NMF algorithms, the iterative process involves additive- or multiplicative-based updating methods. However, given shortcomings such as slow convergence speed and relatively long iterative step, we adopt the gradient-projected-based NMF method to optimize the basic algorithm. The experimental results showed that the proposed method can significantly improve the retrieval speed when reaching the precision and recall rates similar to those of the ordinary and multiplication updating-based NMF methods.

This paper is organized as follows: Section 1 provides a brief introduction on content-based medical image retrieval and the existing CBMIR system developed. Section 2 discusses the existing approaches for NMF decomposition and presents how the multiplicative update and gradient-projected methods work. Section 3 presents the experiments on NMF decomposition and compares the performances of the three methods, and discussions are also drawn in this section. Section 4 provides the conclusions and future works.

2. Proposed Method

2.1 NMF

For a given non-negative $n \times m$ matrix V and a positive integer r, the NMF algorithm can find a non-negative $n \times r$ matrix W and another non-negative $r \times m$ matrix H, subject to $V \approx WH$, and this formula can be rewritten in the form of column vector: $v \approx Wh$.

where v and h are the corresponding column vectors in V and H. Each data vector v is approximately equal to the linear combination of column vector W weighted by the components of h. This condition shows that W is considered a basic matrix and can be used to represent matrix V approximately by linear combination. In other words, a small number of basic vectors can be used to represent a large number of data vectors, and only when the basic vectors are reasonably enough for the structure of data distribution of V can the satisfactory results be reached. Given that negative elements are not allowed in W and H, only the addition operations are permitted, and any subtraction operations are not allowed in representing the whole by parts. This condition reflects the intuitive understanding about showing whole by parts.

Generally, two evaluation functions can be used to estimate the degree of proximity between V and WH. First is the Euclidean distance function:

$$\min_{W,H} f(W,H) \equiv \frac{1}{2}\sum_{i=1}^{n}\sum_{j=1}^{m}(V_{ij} - (WH)_{ij})^2 \quad (1)$$
$$subject\ to\ W_{ia} \geq 0, H_{bj} \geq 0, \forall i,a,b,j$$

The summation in Formula (1) can be rewritten in the form of norm as follows:

$$\sum_{i=1}^{n}\sum_{j=1}^{m}(V_{ij} - (WH)_{ij})^2 = \left\|V - WH\right\|_F^2 \quad (2)$$

This function takes the Euclidean distance between V and WH to evaluate the degree of proximity. Second is the Kullback–Leibler divergence function:

$$\min_{W,H} \sum_{i=1}^{n}\sum_{j=1}^{m}\left(V_{ij}\log\frac{V_{ij}}{(WH)_{ij}} - V_{ij} + (WH)_{ij}\right) \quad (3)$$
$$subject\ to\ W_{ia} \geq 0, H_{bj} \geq 0, \forall i,a,b,j$$

The Kullback–Leibler divergence function is used to evaluate the degree of proximity between V and WH. As far as the second evaluation function is concerned, the function makes no sense when $V_{ij} = 0$ or $(WH_{ij}) = 0$. Thus, we adopt the first function in this study.

2.2 NMF Iterative Method

The multiplicative update and the gradient-projected methods adopted in this study are mainly discussed in this section.

2.2.1 Multiplicative Update Rule

Lee and Seung proposed the most commonly used multiplicative update method [13][14][15] in 2001. The algorithm is as follows:

$$W_{ia}^{k+1} = W_{ia}^{k} \frac{(V(H^k)^T)_{ia}}{(W^k H^k (H^k)^T)_{ia}} \quad \forall i,a$$

$$H_{bj}^{k+1} = H_{bj}^{k} \frac{((W^{k+1})^T V)_{bj}}{((W^{k+1})^T W^{k+1} H^k)_{bj}} \quad \forall b,j \tag{4}$$

Lee and Seung proved that Formulas (4) and (5) are convergent, but W_{ia} and H_{bj} should be strictly positive. If W_{ia} equals 0 in the k^{th} iteration, then all W_{ia} should be 0 in the forthcoming update progress.

The computational complexity should be considered. Both $V(H^k)^T$ and $(W^{k+1})^T V$ are conducted under the complexity level of in Formulas (4) and (5). The denominator in (4) can be transformed to the form of $(WH)H^T$ or $W(HH^T)$ to calculate, as can be seen, the former costs $O(nmr)$ and the latter costs $O(max(m, n) r^2)$, in that $r < min(m, n)$. Thus, the latter is quicker. Similarly, $(W^T W)H$ is adopted in Formula (5). Thus, the cost of calculation for the multiplicative update method is $\#\text{iterations} \times O(nmr)$.

2.2.2 Gradient-Projected Method

The method we considered for matrix updating of W and H is fixing one matrix and altering another:

$$W^{k+1} = \arg\min_{W \geq 0} f(W, H^k) \tag{6}$$

$$H^{k+1} = \arg\min_{H \geq 0} f(W^{k+1}, H) \tag{7}$$

Formulas (6) and (7) can be regarded as sub-problems. Formula (7) can be rewritten as column vector in the following form [16] [17]:

$$H^{k+1,j} = \min \left\| v - W^{k+1} h \right\|^2, h \geq 0 \tag{8}$$

where $H^{k+1,j}$ means the j^{th} column in H^{k+1}.

The border constraint optimization problem should be introduced in the gradient-projected method. The standard border optimization problem is similar to the following form:

$$\min_{x \in R^n} f(x) \quad subject\ to\ l_i \leq x_i \leq u_i, i = 1, \cdots, n \tag{9}$$

Suppose k represents the iteration number, the gradient projected method updates x_{k+1} from x_k using the following rules:

$$x_{k+1} = P[x_k - \alpha \nabla f(x_k)]$$

$$P[x_i] = \begin{cases} x_i & \text{if } l_i < x_i < u_i \\ u_i & \text{if } x_i \geq u_i \\ l_i & \text{if } x_i \leq l_i \end{cases} \tag{10}$$

where the choosing of step a_k is a key point. We adopt a simple and effective method proposed by Dimitri [18]:

Let $0 < \beta < 1$, $0 < \sigma < 1$, initialize x_1, and set $\alpha_0 = 1$, $k = 1, 2, \ldots, N$.

$$x_{k+1} = P[x_k - \alpha_k \nabla f(x_k)] \tag{11}$$

$$f(x_{k+1}) - f(x_k) \leq \sigma \nabla f(x_k)^T (x_{k+1} - x_k) \tag{12}$$

(1) Let $\alpha_k \leftarrow \alpha_{k+1}$.

(2) If α_k satisfies Formulas (11) and (12), then α_k is updated with α_k / β and stopped when α_k does not satisfy (11) and (12) or $x(\alpha_k / \beta) = x(\alpha_k)$. Otherwise, α_k is updated with α_k / β and stopped when α_k does not meet the conditions.

Focusing back on NMF, Formula (7) can be rewritten for convenience.

$$\min_H \bar{f}(H) \equiv \frac{1}{2} \|V - WH\|_F^2 \quad subject\ to\ H_{bj} \geq 0, \forall b, j \tag{13}$$

where both V and W are constant matrices in (13), which can be rewritten in vector form as follows:

$$\bar{f}(H) = \frac{1}{2} \|V - WH\|_F^2 = \frac{1}{2} vec(H)^T \begin{bmatrix} W^T W & & \\ & \ddots & \\ & & W^T W \end{bmatrix} vec(H) + H'\text{s linear terms} \tag{14}$$

The Hessian matrix in $\bar{f}(H)$ is block diagonal. In fact, each block $(W^T W)$ is a $r \times r$ positive semidefinite matrix. Given that $W \in R^{n \times r}$ and $r << n$, $(W^T W)$ and the whole Hessian matrix are well-conditioned, which is a good property in optimization algorithm, and rapid convergence can be guaranteed.

Solving sub-problems (6) and (7) in each step of the iterative process is time consuming because each sub-problem requires an iterative process that can also be regarded as a sub-iteration. When the gradient-projected method is used to solve (13), gradient $\nabla \bar{f}(H) = W^T (WH - V)$ needs to be calculated in each iteration.

Based on the discussion in Section 2.2.1, reducing the computational complexity is possible by calculating $(W^T W)H$ - $W^T V$, in which $W^T W$ and $W^T V$ cost $O(nr^2)$ and $O(nmr)$, respectively.

Formula (12) can be implemented by searching for step

α, but it is time consuming. Suppose $\bar{H}$ and $\tilde{H}$ are the current and next rounds of the iterative value respectively, can be returned by calculating $\tilde{H} \equiv P[\bar{H} - \alpha\nabla\bar{f}(\bar{H})]$, and $\bar{f}(\bar{H})$ cost $O(nmr)$. If t times of experiments exist, then the computational complexity, $O(tnmr)$, for these operations would be enormous. Thus, we adopt the following method to reduce the amount of calculation. For a quadratic function $f(x)$ and any given vector $\vec{d}$:

$$f(x+\vec{d}) = f(x) + \nabla f(x)^T \vec{d} + \frac{1}{2} d^T \nabla^2 f(x) \vec{d} \quad (15)$$

Thus, Formula (12) can be rewritten as follows:

$$\begin{aligned} &(1-\sigma)\nabla f(\bar{x})^T(\bar{x}-\tilde{x}) \\ &+\frac{1}{2}(\bar{x}-\tilde{x})^T \nabla^2 f(\bar{x})(\bar{x}-\tilde{x}) \le 0 \end{aligned} \quad (16)$$

As for $\bar{f}(H)$ in (13), (12) transforms to the following:

$$\begin{aligned} &(1-\sigma) \ < \nabla\bar{f}(\bar{H}), \tilde{H}-\bar{H} > \\ &+\frac{1}{2} \ < \tilde{H}-\bar{H}, (W^T W)(\tilde{H}-\bar{H}) > \ \le 0 \end{aligned} \quad (17)$$

The inclusions in angle brackets in Formula (17) are the inner products for two matrices, and the main part of the computation for (17) is $(W^T W)(\tilde{H} - \bar{H})$, which costs $O(mr^2)$. Thus, the amount of computation for (12) changes from $O(tnmr)$ to $O(tmr^2)$. Combined with the $O(nmr)$ of $(W^T V)$. mentioned, the total cost for solving Formula (13) using the gradient-projected method is $O(nmr)$ + #sub - iterations $\times$ $O(tmr^2)$.

Based on the abovementioned facts, Formula (6) can be rewritten as follows:

$$\bar{f}(W) \equiv \frac{1}{2}\left\| V^T - H^T W^T \right\|_F^2 \quad (18)$$

where V^T and H^T are constant matrices. Thus, the amount of computation complexity for (18) is $O(nmr)$ + #sub - iterations $\times$ $O(tnr^2)$. The total computation complexity is # iterations $\times$ ($O(nmr)$ + #sub - iterations $\times$ $O(tmr^2 + tnr^2)$). Given that #sub - iterations and t are relatively small, the amount of computation is much lower than that of the multiplicative method.

2.2.3 Stop Condition

In boundary constraint optimization problems, a general method to identify whether point x_k is close enough to the stagnation point can be determined by Formula (19):

$$\left\| \nabla^P f(x_k) \right\| \le \varepsilon \left\| f(x_1) \right\| \quad (19)$$

where ε is the tolerance degree, and $\nabla^P f(x_k)$ is the gradient projection and is defined as follows:

$$\nabla^P f(x)_i \equiv \begin{cases} \nabla f(x)_i & \text{if } l_i < x_i < u_i \\ \min(0, \nabla f(x)_i) & \text{if } x_i = l_i \\ \max(0, \nabla f(x)_i) & \text{if } x_i = u_i \end{cases} \quad (20)$$

With regard to the NMF problem, (19) transforms to the following form:

$$\left\| \nabla^P f(W^k, H^k) \right\|_F \le \varepsilon \left\| \nabla f(W^1, H^1) \right\|_F \quad (21)$$

The sub-iterations in sub-problems (6) and (7) also require a stop condition, and it can be achieved by the following discriminants:

$$\begin{aligned} \left\| \nabla_W^P f(W^{k+1}, H^k) \right\|_F &\le \bar{\varepsilon}_W \\ \left\| \nabla^P f(W^{k+1}, H^{k+1}) \right\|_F &\le \bar{\varepsilon}_H \end{aligned} \quad (22)$$

Let

$$\bar{\varepsilon}_W = \bar{\varepsilon}_H \equiv \max(10^{-3}, \varepsilon) \left\| \nabla f(W^1, H^1) \right\|_F \quad (23)$$

If the process in Sub-problem (6) stops without the occurrence of any iteration, then the tolerance is decreased by $\bar{\varepsilon}_W \leftarrow \bar{\varepsilon}_W / 10$, and the process iteration is continued. Sub-problem (7) can be treated in the same manner.

3. Experiments

The NMF algorithm is employed in medical image retrieval experiments. Suppose a total of n images are annotated by users and are regarded as positive samples, and the original data matrix V can be constituted by the characteristic vectors of these n images. In the training process, the base matrix W and the coefficient matrix H of the training samples are obtained, and the inquiry feature $h_{inquiry}$ under the new space can also be achieved. V_{all} is then generated by the characteristics of all images in the database. W is considered the base matrix, and NMF decomposition is conducted to obtain the coefficient matrix H_{all}. The column vector of is considered the feature vector of the image under the space of base matrix W, and the distance between the feature vector under the new space and the new inquiry feature $h_{inquiry}$ is obtained to measure the similarities of images. Finally, N images with the highest similarity values are returned after sorting.

The experiment was conducted under image databases of 586 cerebral hemorrhage images and 634 spine and cervical-spine mixed images to test the performance of the NMF relevance feedback. The image features, such as gray, texture, and resolution, are adopted as the original characteristics. The entire experiment is implemented under the CBMIR system developed by our project members.

3.1 Experimental Parameters

Two important parameters must be determined in the NMF decomposition process, namely, the number of columns

r for base matrix W and the maximum number of iterations ε, which is the calculation error in the stop condition of iteration, is also necessary. Based on the experiments, we found that $r = 2$ can result in best effects of the feedback. Thus, the maximum number of iterations is initialized as 10000, and ε is selected as 10^{-6} experientially.

3.2 Experimental Results

3.2.1 Retrieval Performance Comparison

We adopt precision and recall rates in the experiment to evaluate the performance of the feedback system and set the returning images as 0, 5, … , 95, 100 with an interval of 5. For each of the returning image groups, 20 images are selected, and the retrieval experiments are conducted on these images. The precision and recall of the 20 images should be averaged and appear as the precision and recall for the corresponding image group. These factors are used to generate the curves further on.

In Fig. 1, axis Y represents precision, and axis X describes the number of returning images. As the number of returning images increases, the precision rates for all methods decrease. The precision of the gradient-projected method is slightly superior to the multiplicative update method, and both methods are significantly higher than the ordinary retrieval method. This result is partly due to the improvement on the base of the ordinary one by the algorithms of the two methods. In Fig. 2, axes X and Y represent the recall and number of returning images, respectively. As the number of returning images increases, the recall rate increases. However, the gradient-projected method is always beyond the other two approaches at each of the label in axis X. In Fig. 3, sub-image (a) represents the query image, and sub-images (b)–(d) display the retrieval results of the three methods in our experiment. If the checkbox below those images are blank, then they are the relevant feedback images that are retrieved by the system, and the images with a white background and a ticked checkbox are irrelevant. The figure also shows that (b) and (c) achieve the same results, that is, six images are irrelevant from the image library, and (d) only has two irrelevant images. Thus, from the point of retrieval image numbers, the gradient-projected method surpasses the other two methods.

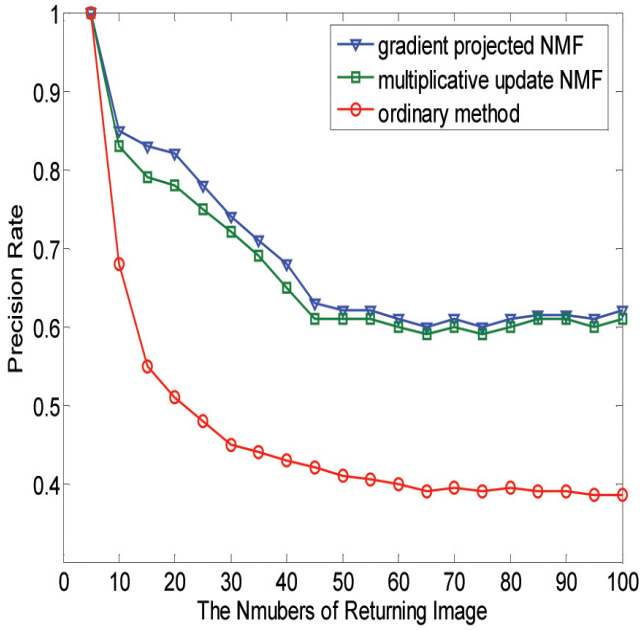

Figure 1. Average precision rate curve for cerebral hemorrhage MR (Magnetic Resonance) images

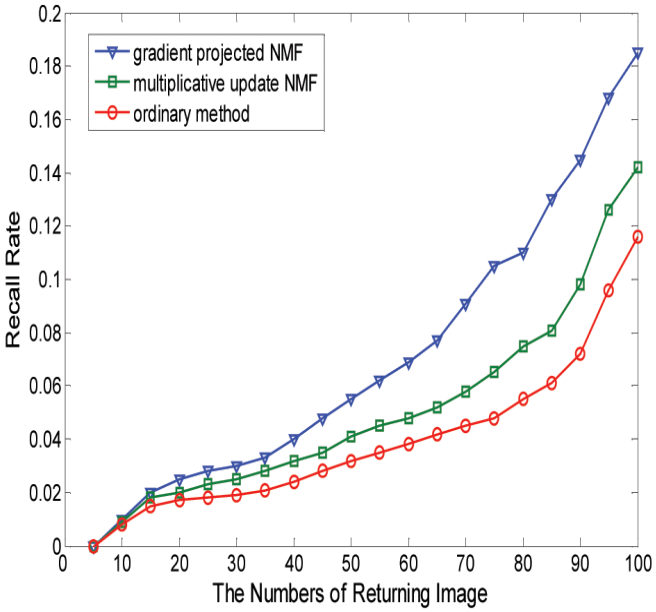

Figure 2. Average recall rate curve for cerebral hemorrhage MR images

We illustrate the results of another group of experiments to verify the effects of our method. Fig. 4 shows that the query image is a spine image, that is, users want to query images related to the spine in various views. Thus, (a) is a spine image, and (b)–(d) display the retrieval results on three different methods. The three approaches can retrieve the images that correspond to the spine category.

However, some spine images in sub-images (b)–(d) are not really the true spine, but are just similar to the spine. For example, the three methods can retrieve the results that look like the query image, but some ticked images in (b)–(d) are cervical spine images, bone with bandage, and some other images. We adopt the same strategy used in Figure 3, that is, the images with an unticked checkbox are relevant feedback images to the query image, and those with a white background and a ticked checkbox are irrelevant, as shown in (b)–(d). The figure shows that (b) and (c) also obtain the same results, namely, six varied irrelevant images are retrieved based on our image database, and (d) has three irrelevant images. These results are partly due to the similar anatomical structural view of the spine and the cervical spine. Thus, our future work will focus on how to improve the retrieval accuracy of these two spines. The gradient-projected method in sub-image (d) contains the least irrelevant images. Thus, the proposed method can retrieve more relevant images and is effective and feasible.

(a) Query image

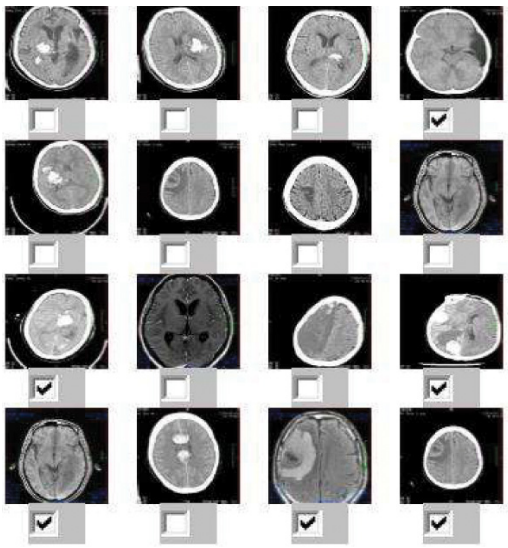

(b) Ordinary method

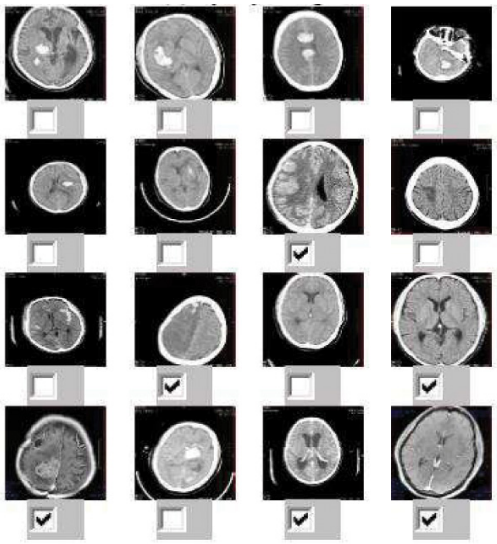

(c) Multiplicative update NMF

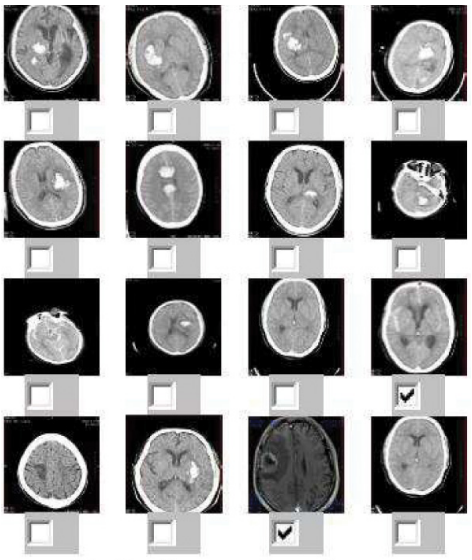

(d) Gradient-projected NMF

Figure 3. Comparison of the three methods on cerebral MR image retrieval

(a) Query image

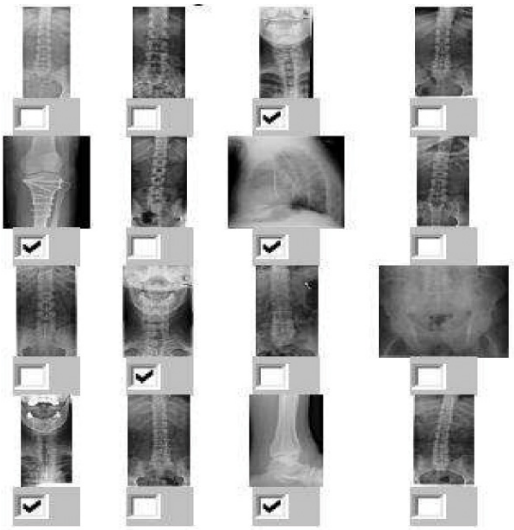

(b) Ordinary method

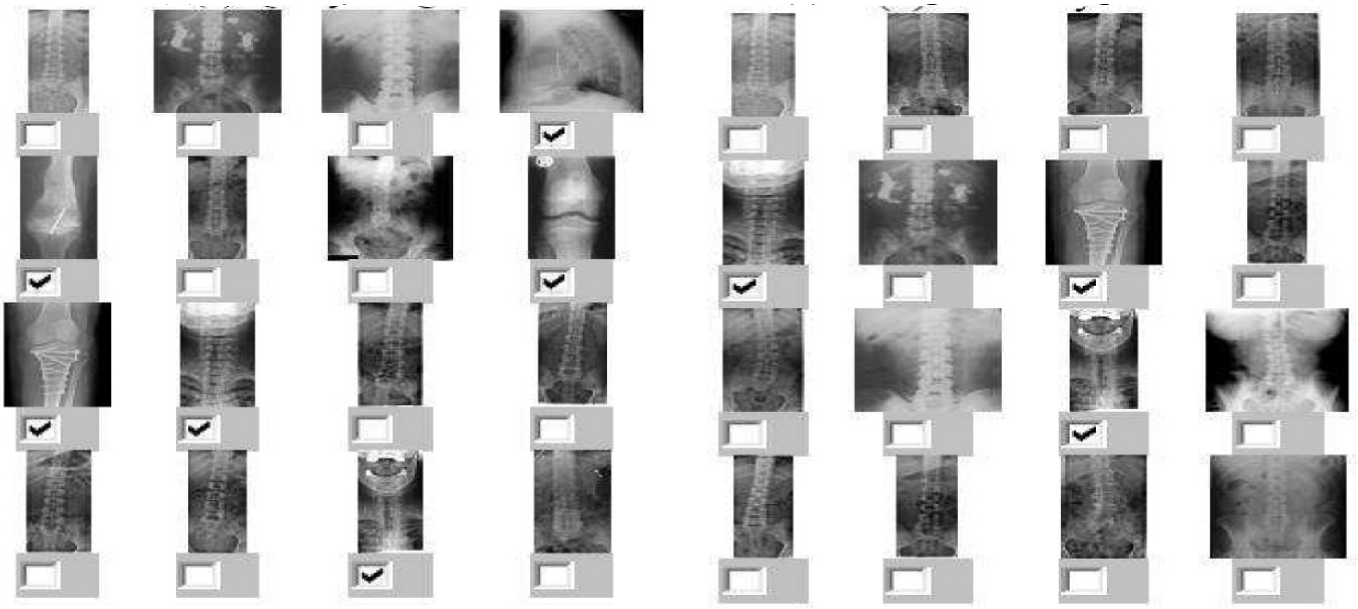

(c) Multiplicative update NMF (d) Gradient-projected NMF

Figure 4. Comparison of the three methods on spine X-ray image retrieval

3.2.2 Feedback Time

The feedback speed for the multiplicative and gradient-projected NMF algorithms is compared, and 20 images are adopted to calculate the elapsed time and number of iterations. Each selected image is estimated by both methods, and the average results are displayed in Table 2. The table shows that the gradient-projected method is superior to the multiplicative NMF method because both the number of iterations and time consumption are significantly decreased.

Feedback model	Number of iterations	Names of the System
Multiplicative NMF	5327	1.3689
Gradient-projected NMF	58	0.1253

Table 2. Performance Comparison of Two Methods

4. Conclusion

Medical image retrieval with different collecting devices is conducted in this study. The two groups of experiments, MR and X-ray, indicate that the NMF method can be employed in the relevance feedback process for image retrieval. The relevant images will be annotated before they are used as training samples and are decomposed under the NMF operation, and the base and coefficient matrices are obtained. The feature vectors of all images in the image library are used to create a new data matrix and conduct NMF decomposition based on the base matrix to obtain the corresponding coefficient matrix. As a result, efficiently retrieving more relevant images is possible. Applying the gradient-projected method in NMF decomposition can significantly reduce the calculation complexity from the time-cost standpoint when compared with the ordinary and traditional multiplication updating method. The initialization of the base matrix W and coefficient matrix H is randomly provided in the experiments, and r, the column of the base matrix, is empirically obtained in the experiment instead of by any existing standard. Our future research will focus on how to initialize W and H and how to determine the value of r.

5. Acknowledgment

This work is supported by A Major Project of Education Department in Sichuan China (Grant No. 14ZA0124). The authors would like to thank the anonymous reviewers for their useful comments and suggestions.

References

[1] Müller, H., Michoux, N., Bandon, D., et. al (2004). A review of content-based image retrieval systems in medical applications—clinical benefits and future directions. *International Journal of Medical Informatics*, 73 (1) 1-23.

[2] Burdescu, D.D., Mihai, C.G., Stanescu, L., et. al (2013). Automatic image annotation and semantic based image retrieval for medical domain. *Neurocomputing*, 109 (3) 33-48.

[3] Dankerl, P., Cavallaro, A., Tsymbal, A., et. al (2013). A retrieval-based computer-aided diagnosis system for the characterization of liver lesions in CT scans. *Academic Radiology*, 20 (12) 1526-1534.

[4] Li, L., Zhang, Q. Z., Ding, Y. H., et. al (2014). Automatic diagnosis of melanoma using machine learning methods on a spectroscopic system. *Bio-med Central Medical Imaging*,14 (36) 1-12.

[5] Adgaonkar, A., Atreya, A., Akshay, D., et. al (2014).

Identification of tuberculosis bacilli using image processing. *In:* Proceedings on International Conference on Electronics & Computing Technologies, International Journal of Computer Applications, 25-28.

[6] Cho, H.C., Hadjiiski, L., Sahiner, B. (2011). Similarity evaluation in a content-based image retrieval (CBIR) CADx system for characterization of breast masses on ultrasound images. *Medical Physics*, 38 (4) 1820-1831.

[7] Quellec, G., Lamard, M., Cazuguel, G. (2010). Adaptive nonseparable wavelet transform via lifting and its application to content-based image retrieval. *IEEE Transactions on Image Processing*, 19 (1) 25-35.

[8] Pilevar, A. H. (2011). Content-based image retrieval algorithm for medical image databases. *Journal of Medical Signals and Sensors*, 1 (1) 12-18.

[9] Edmundson, D., Schaefer, G. (2012). Fast JPEG image retrieval using tuned quantisation tables. *In: Proceeding of IEEE International Conference on Signal Processing, Communication and Computing*, IEEE Publishing, 234-239.

[10] Tsuge, S., Shishibori, M., Kuroiwa, S., et. al (2001). Dimensionality reduction using non-negative matrix factorization for information retrieval. *In: IEEE International Conference on Systems, Man and Cybernetics*, IEEE Publishing, 960-965.

[11] Li, Y., Geng, B., Tao, D., et. al. (2012). Difficulty guided image retrieval using linear multiple feature embedding. *IEEE Transactions on Multimedia*, 14 (6) 1618-1630.

[12] Lee, D. D., Seung, H. S. (1999). Learning the parts of objects by non-negative matrix factorization. *Nature*, 401(6755) 788-791.

[13] Chih, J. L. (2007). Methods for non-negative matrix factorization. *Neural Computation*, 2756-2779.

[14] Kumar, A., Kim, J. M., Cai, W. D., et. al. (2013). A content-based medical image retrieval: A survey of applications to multidimensional and multimodality data. *Journal of Digital Imaging*, 26 (6) 1025-1039.

[15] Kitanovski, I., Trojacanec, K., Dimitrovski, I. (2012). Multimodal medical image retrieval. *In:* ICT Innovations, Advances in Intelligent Systems and Computing, 81-89.

[16] Fakhari, A., Moghadam, A. M. E. (2012). Combination of classification and regression in decision tree for multi-labeling image annotation and retrieval. *Applied Soft Computing*, 13 (2) 1292-1302.

[17] Quellec, G., Lamard, M., Cazuguel, G. (2012). Fast wavelet-based image characterization for highly adaptive image retrieval. *IEEE Transactions on Image Processing*, 21 (4) 1613-1623.

[18] Dimitri, P. B (1999). Non-linear Programming. Nashua USA, Athena Scientific 2nd ed. 136-145